

Medium Effects on the Electron Transfer Reaction Between Excited Singlet Pyrene and Indole

*Marcela S. Altamirano, Claudio D. Borsarelli, Héctor A. Garrera, Hernán A. Montejano, Teresa Quintero, Juan J. Cosa and Carlos M. Previtali**

*Departamento de Química y Física, Universidad Nacional de Río Cuarto,
5800 Río Cuarto, Argentina*

Received: September 14, 1994

A cinética da transferência de elétrons entre derivados de pireno no estado singlete excitado e indóis foi estudada em vários meios. Em soluções homogêneas, a constante de velocidade bimolecular aumenta com a constante dielétrica macroscópica do solvente. Isto parece representar um comportamento geral, independente da estrutura microscópica do solvente exceto para os supressores mais eficientes, nos quais a contribuição difusional se torna importante. A eficiência da separação de cargas também foi investigada em soluções homogêneas. Foi encontrado que as variações observadas podem ser explicadas pela tendência da constante de escape da gaiola, de acordo com o modelo de Eigen. A etapa de transferência de elétrons é seguida, em alguns casos, por uma transferência de prótons, que leva a uma reação fotoquímica. Foi investigado o efeito de micelas normais sobre estas reações. Também foi estudado o efeito de micelas reversas e polieletrólitos sobre a eficiência da supressão. Foi encontrado que a reação pode ser controlada usando derivados do supressor e da molécula excitada que estejam localizados em regiões conhecidas do sistema organizado.

The kinetics of the electron transfer reaction between excited singlet pyrene derivatives and indoles has been investigated in several media. In homogeneous solvents the bimolecular rate constant increases with the solvent macroscopic dielectric constant. This seems to be a general behavior independent of the solvent microscopic structure, except for the most efficient quenchers in which the diffusional contribution becomes important. The charge separation efficiency was also investigated in homogeneous solvents. It was found that the changes observed may be explained by the trend in the cage escape rate constant according to the Eigen's model. The electron transfer step in some cases is followed by a proton transfer process which leads to a photochemical reaction. The effect of normal micelles on this reaction was investigated. Also the effect of reverse micelles and polyelectrolytes on the efficiency of the quenching was studied. It was found that the reaction can be controlled by employing derivatives of both the quencher and quenchee that are localized in known regions of the organized system.

Keywords: *electron transfer, medium effects, pyrene*

Introduction

The quenching of the excited singlet state of pyrene by indolic compounds has been the subject of several studies both in homogeneous^{1,2} and microheterogeneous³⁻⁵ solution. In non-polar solvents, indole derivatives have been shown to form emissive exciplexes with pyrene and 1-cyanopyrene¹. In polar solvents the bimolecular quenching rate constant increases with the solvent polarity⁴ becoming near diffusion controlled in water. The electron transfer

nature of the quenching process has been confirmed by laser flash photolysis experiments² and the solvent effect on the quantum yield of charge separation was measured. It was also observed that a photochemical reaction which leads to the consumption of pyrene takes place in homogeneous solvent with a fair efficiency. In micellar solutions the quenching of pyrene by indole and tryptophan was employed by Lissi and Encinas^{4,5} for the determination of the partition coefficient of the indolic compounds. The reaction presents several aspects of interest from the point

of view of the medium effects on electron transfer reactions. In this paper we present results on the solvent effects on the kinetics parameters and quantum yields and how the reaction is affected when it is carried out in microheterogeneous systems such as normal and reverse micelles. The effect of polyelectrolytes on the system was also investigated. The reaction was studied between unsubstituted pyrene and indole and also with the derivatives shown in Scheme 1.

Experimental

The solvents acetone, acetonitrile MeCN and MeOH were Sintorgan HPLC grade, and were used without further purification. EtOH was distilled twice before use. Propionitrile (PrCN) was from Fluka; and was distilled and passed through a silica-gel column before use. Pyrene (Py) from Merck was purified by recrystallization from methanol. Indole (In) and its derivatives were obtained from Sigma and used without further purification. Pyrene derivatives were from Molecular Probes. The surfactants sodium dodecylsulfate (SDS) and cetyltrimethylammonium chloride (CTAC) were recrystallized previous to use. AOT was from Sigma and used as received. It was verified that the

absorption and emission intensities of the detergents were negligible at the wavelength ranges of interest.

Stationary fluorescence quenching experiments were carried out with an Fluoromax spectrofluorometer. For transient absorption and fluorescence lifetime determinations, a nitrogen laser (Laseroptics), 5 ns FWHM and 5 mJ per pulse, was employed. For fluorescence measurements the laser beam was highly attenuated. The sample was placed in a TRW 75A filter fluorometer with appropriate filters. The signal was acquired by a digitizing scope where it was averaged and then transferred to a computer. The samples were deoxygenated by nitrogen bubbling for at least 15 min.

Quantum yields of pyrene triplet state and radical anions were determined by the laser flash photolysis technique. Since photoexcited pyrene readily reacts with indole, specially in MeCN, the solutions were changed after exposure to a few laser pulses.

Results and Discussion

Solvent effects on the forward electron transfer rate constant

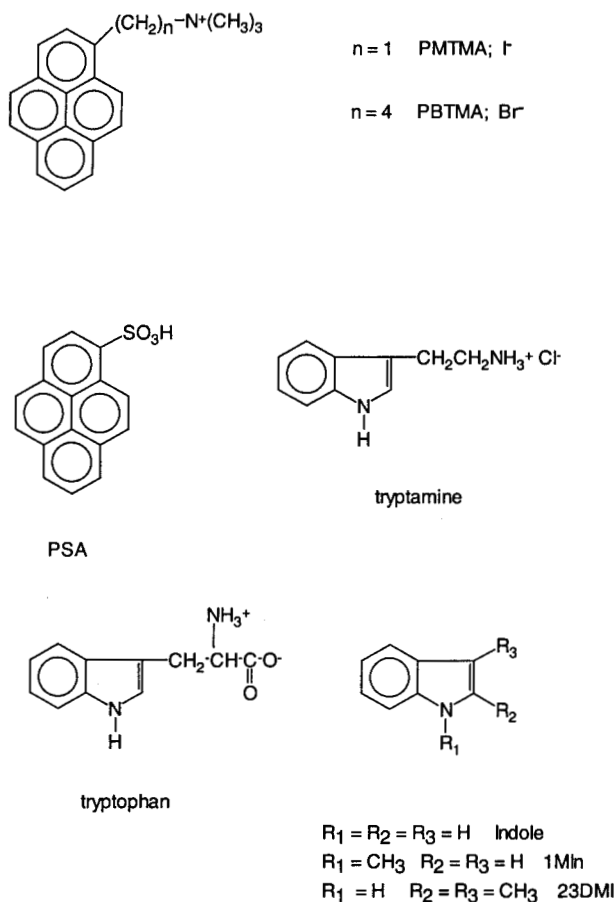
In spite of the large amount of work on photoinduced electron transfer reactions the solvent effect on the rate constants of intermolecular processes has received little consideration until recently. There remain several aspects of these effects that are not satisfactorily explained by the simple Rehm-Weller-Marcus model. Some of the difficulties encountered are exemplified by the system pyrene-indole.

The interaction between singlet excited pyrene and indoles can be discussed on the basis of the mechanism shown in Scheme 2.

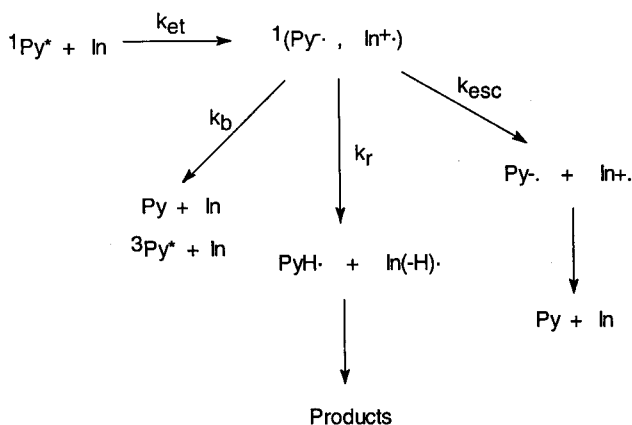
Rate constants k_{et} for the quenching of $^1\text{Py}^*$ by In were obtained by measuring the fluorescence lifetime τ , as a function of the indole concentration. For some systems the results were checked by stationary fluorescence quenching experiments. The decay of $^1\text{Py}^*$ in the presence of In was monoexponential in all the homogeneous solvents here investigated. The results were plotted according to Eq. 1.

$$\tau^{-1} = \tau_0^{-1} + k_q [\text{In}] \quad (1)$$

where τ_0 is the fluorescence lifetime in the absence of In. Linear plots were obtained in all cases and the results are collected in Table 1 for the unsubstituted pyrene-indole system. Exciplex emission was not observed in any of the solvents employed, even at the higher quencher concentration. The electron transfer nature of the quenching process was confirmed by the transient absorption spectra of the long lived species remaining after the quenching event. These spectra are shown in Fig. 1 for four solvents. In the absence of indole the only transient absorption present corresponds to the triplet state of pyrene. In the presence of indole the typical spectrum of the pyrene radical anion ($\lambda_{\text{max}} = 490 \text{ nm}$) can be observed in all cases.



Scheme 1.



Scheme 2.

Table 1. Rate constants and free ion quantum yields for the electron transfer quenching of pyrene excited singlet by indole.

Solvent	τ_0/ns	$k_q/\text{M}^{-1}\text{s}^{-1}$	Φ_{ion}	ϵ (dielectric constant)
MeCN	338	2.4×10^8	0.37 ± 0.02	35.9
MeOH	320	1.5×10^8	0.22 ± 0.02	32.7
PrCN	368	1.1×10^8	0.24 ± 0.04	28.9
EtOH	384	6.4×10^7	0.04 ± 0.01	24.6
Acetone	345	4.8×10^7	0.16 ± 0.02	20.6

The effect of the macroscopic dielectric constant of solvent mixtures on k_{et} was also investigated. In Fig. 2 the quenching rate constant of several pyrene derivatives by indole is plotted vs. the dielectric constant of EtOH-water mixtures. It can be seen that for the case of Py and PBTMA the rate constant increases with the solvent polarity. Encinas and Lissi⁴ also observed previously this effect in the case of the unsubstituted system. For the other pyrene derivatives, PMTMA and PSA, and for some methyl substituted indoles (not shown in the plot) the rate constants are higher and near solvent independent. For these cases the rate constants are close to the diffusional limit, 6.5×10^9 and $5.4 \times 10^9 \text{ M}^{-1} \text{ s}^{-1}$ in water and ethanol, respectively. Therefore, they become independent of the solvent polarity. The reason for the near diffusion controlled rate constants may be found in a higher donor capability of the indole derivative due to the methyl substitution of the heterocyclic ring, or in a solvation shell of the pyrene ring with a larger water content due to the charge proximity in the case of PSA and PMTMA.

The strong dependence of the rate constant upon the dielectric constant for Py-In and PBTMA-In can not be explained by the current models of electron transfer kinetics. In the classical Marcus electron-transfer theory⁶ the rate constant for a bimolecular electron transfer proceeding by the following simple mechanism:

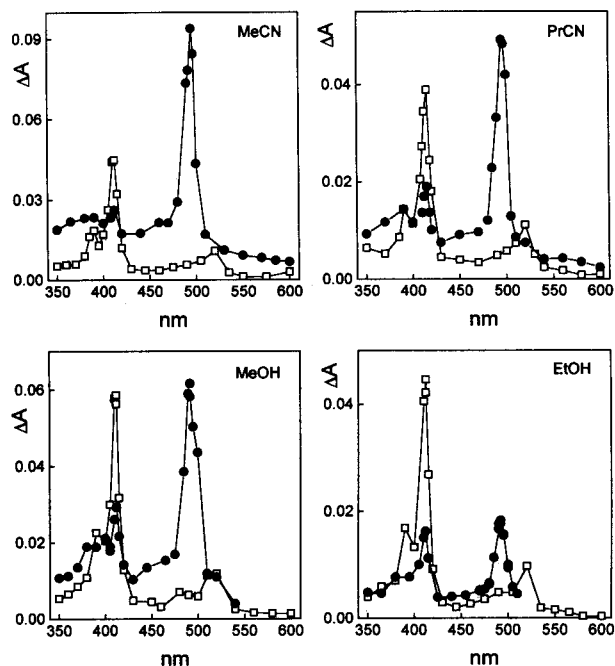


Figure 1. Transient absorption spectra of pyrene in the absence (\square) and the presence of indole (\bullet) taken $1\mu\text{s}$ after the laser pulse. The indole concentration is such that the fraction of excited singlets quenched is 0.93 in MeCN, 0.90 in PrCN, 0.88 in MeOH, and 0.87 in EtOH.

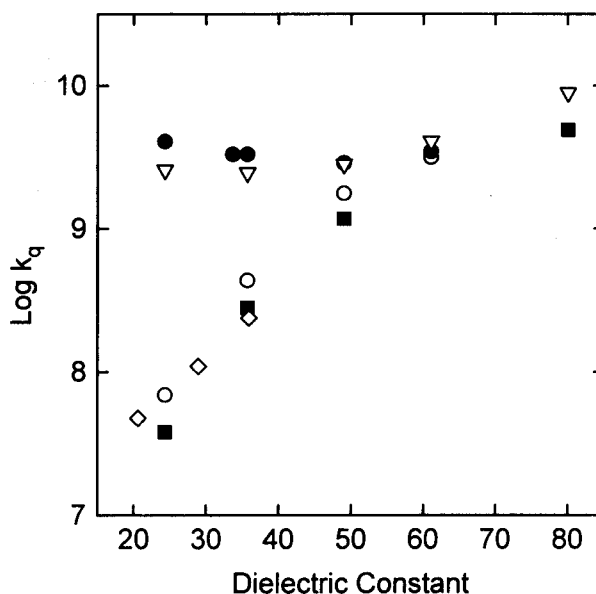
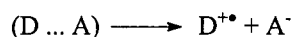


Figure 2. Quenching rate constants as a function of the solvent dielectric constant for: (\blacksquare) = PBTMA-In in EtOH-water; (\circ) = Py-In in EtOH-water (Ref. 4); (\diamond) = Py-In in alkylnitriles and acetone; (\bullet) = PMTMA-In in EtOH-water; (∇) = PSA-In in EtOH-water.



is given by⁶:

$$k_{et} = K_D \kappa_{el} \nu_n \exp\left(-\frac{(\lambda + \Delta G^\circ)^2}{2 \lambda R T}\right) \quad (2)$$

where K_D is the equilibrium constant for the formation of the encounter complex, ν_n is a nuclear frequency of passage through the transition state, and κ_{el} is the electronic transmission coefficient. In the classical treatment κ_{el} is usually taken as unity. ΔG° is the Gibbs energy of the electron transfer reaction when the donor and acceptor are at a distance r_{AD} .

The reorganization energy λ has two contributions:

$$\lambda = \lambda_{in} + \lambda_{out} \quad (3)$$

The inner term λ_{in} arises from structural changes on going from the equilibrium configuration of the reactants to that of the products. It is a function of bond lengths and force constants in both states. The outer term λ_{out} is called the solvent reorganization energy and it is often the major contribution to the total reorganization energy. When a dielectric continuum model is applied, the solvent contribution can be written as⁶:

$$\lambda_{out} = B \left[\frac{1}{\epsilon_{op}} - \frac{1}{\epsilon_s} \right] = B \gamma \quad (4)$$

where ϵ_{op} and ϵ_s are respectively the optical and static dielectric constants, and B is a function of the model and molecular dimensions that are usually taken as solvent independent.

According to Marcus classical theory the solvent may influence the electron transfer rate constant by altering several of the parameters involved. First, the driving force ΔG° may be altered by different stabilization of the product ion pair. Second, the solvent contribution to the reorganization energy λ_{out} is modified through changes in the static and optical dielectric constants. Finally, the nuclear frequency may be expected to be solvent dependent if it is predominantly a solvent mode⁷. For the solvents under consideration, γ in Eq. 4 is practically the same (0.493 for acetone, 0.523 for MeCN, 0.501 for PrCN, 0.499 for EtOH, 0.536 for MeOH, and 0.550 for water at room temperature) and the driving force for a given reaction is not expected to differ significantly from one solvent to another, at least not to produce a change of two orders of magnitude in the rate constant. Therefore the observed solvent effects on the rate constants can not be explained by changes in the exponential term if a continuum model of the solvent is considered. In the preexponential term of Eq. 2, K_D is at a first approximation solvent independent, and consequently the nuclear frequency might be the main factor responsible for the changes in the rate constant. In order to disentangle the solvent effect on the preexponential term, studies of the

temperature effects on the rate constants are needed. They were performed for the system Py-In in some solvents², and it was found that both the frequency factor and the exponential term change in a complex fashion. In any case, from a phenomenological point of view it can be said that the macroscopic parameter which governs the kinetic behavior of the Py-In system below the diffusional limit, is the dielectric constant. This is based on the good correlation of the rate constants in aprotic solvent with the dependence in EtOH-water mixtures (See points for MeCN, PrCN and acetone in Fig. 2).

Solvent effects on the charge separation efficiency

In photoinduced electron transfer reactions one of the most important parameters from a practical point of view, is the charge separation efficiency of the process. That is the ability to separate the products of the electron transfer reaction before they collapsed to the starting reactants in their ground state by a back-electron transfer reaction. This efficiency is affected by various factors such as the viscosity and polarity of the solvent, the presence of organized structures such as micelles or the application of an external magnetic field.

The solvent effect on the charge separation process is apparent from the intensity of Py^\cdot peaks in Fig. 1. These spectra were taken under conditions of equal absorption of the laser pulse and the same fraction (90%) of singlet quenching. Two species are predominant in the spectra, the triplet state ($\lambda_{max} = 414 \text{ nm}$) and the pyrene radical anion ($\lambda_{max} = 490 \text{ nm}$). The triplet yields are very much higher than those expected according to the fraction of excited singlet states quenched. Consequently it can be concluded that the quenching process leads in part to the triplet state. The free radical ion quantum yields were determined by relative actinometry, using the triplet state of ZnTPP as actinometer. The results are also collected in Table 1. It can be seen that the yields present large differences from one solvent to another. In the time scale of our laser photolysis experiments, the pyrene radical anions observed are those that escape the cage recombination processes. According to the Scheme 2, the free ions quantum yield can be written as:

$$\Phi_{ion} = f \times \frac{k_{esc}}{k_{esc} + \sum k_d} \quad (5)$$

where f is the fraction of singlets quenched, and $\sum k_d$ stands for the sum of all the decay paths of the geminate radical ion pair, including the reactive and intersystem crossing routes. Eq. 5 can be re-written as:

$$\frac{\Phi_{ion}}{f - \Phi_{ion}} = \frac{k_{esc}}{\sum k_d} \quad (6)$$

Hence a plot of the left hand side vs. k_{esc} should result in a straight line going through the origin. In order to estimate k_{esc} we made use of the Eigen equation⁸:

$$k_{esc} = \left(\frac{2 k_b T}{\pi \eta r^2} \right) \left(\frac{z_A z_B e^2}{\epsilon r k_B T} \right) [1 - \exp(-\frac{z_A z_B e^2}{\epsilon r k_B T})]^{-1} \quad (7)$$

where η and ϵ are the solvent viscosity and dielectric constant, respectively. z_A and z_B are the charges of the separating ions initially at a distance r . Assuming 0.7 nm for r , Eq. 7 affords $6 \times 10^9 \text{ s}^{-1}$ for ${}^1k_{esc}$ in MeCN. This was re-scaled by a factor 1/6 in order to agree with the experimental results in MeCN⁹. A plot of the results of radical ion quantum yield according to Eq. 6 for the system pyrene-indole can be seen in Fig. 3.

Within the experimental error of the data, a linear plot with zero intercept is obtained. It can be concluded that for this system the macroscopic solvent properties give a good account of the observed behavior. Moreover, according to Eq. 6 the linearity of the plot implies a constant value of Σk_d , e.g., the decay of the geminate ion-pairs formed in the excited singlet quenching of pyrene by indole to ground state, triplet state or products, is solvent independent. This result is most remarkable since it is independent of the protic or aprotic nature of the solvent.

Photoreaction and micellar effect on the quantum yield

When Py is irradiated continuously at one of its absorption peaks in the near UV in the presence of Indole, a bleaching of the former is apparent, concomitantly with the appearance of a new broad band shifted to the red (Fig. 4). An isosbestic point can be observed, that may be taken as an indication of a clean photochemical reaction. When transient absorption spectra are taken for the system in homogeneous solvent, it is observed that after the decay of

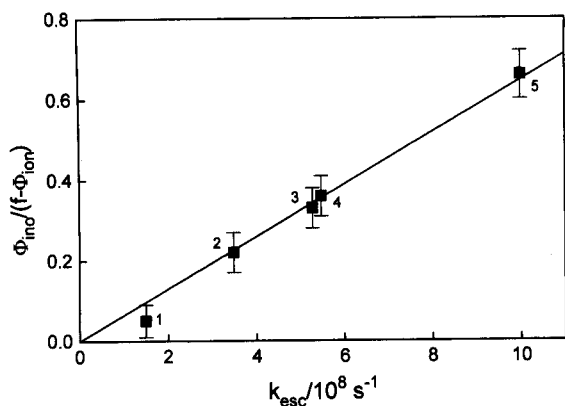


Figure 3. Plot of the left hand side of Eq. 6 vs. the cage escape rate constant k_{esc} calculated by the Eigen model (Eq. 7). Solvents: 1 = EtOH, 2 = Acetone, 3 = MeOH, 4 = PrCN, 5 = MeCN. Error bars result from the experimental errors of Φ_{ion} in Table 1.

the radical ion and the triplet of pyrene, a new band centered near 400 nm persists (Fig. 5). This new band can be ascribed to the hydropyrenyl radical¹⁰. In Fig. 6 the bleaching of the Py band at 334 nm is plotted as a function of time, under different conditions for In itself and the derivative N-methylated 1-MI. It can be seen that when the H-atom on the N-heteroatom is replaced by a methyl group the system is practically photochemically stable. Also a noticeable solvent effect on the rate of bleaching can be observed. Acetone is a more efficient solvent than alcohols for the photoreaction.

The effect of surfactants can be seen in Fig. 7. Both cationic (CTAC) and anionic (SDS) micelles inhibit the photobleaching of Py, while in the neutral Brij-35 micelles it behaves in a similar fashion to that of EtOH. In Fig. 8 the effect of the three surfactants on the radical ion yield is shown. For CTAC micelles at the same time that inhibition of the reaction is observed an enhancement in the free ions yield is apparent. We think that this result can be explained if it is assumed that the reaction mechanism involves a proton transfer step after the initial electron transfer and previous to the separation into free ions (Scheme 2). In this way the hydropyrenyl and indolyl radical are produced. Subsequently, by reaction with the solvent or by recombination at different position, these radicals may give place to the stable photoproducts. The micellar interface of CTAC may preclude the proton transfer step by expelling the indole radical cation from the interface to the water

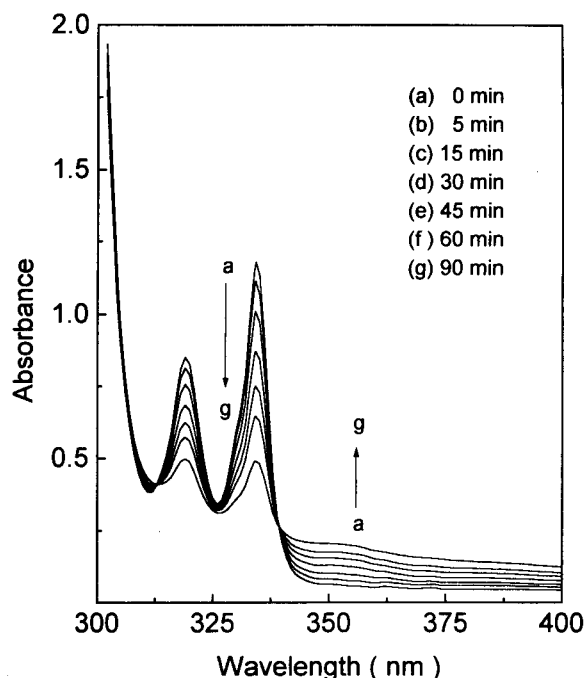


Figure 4. Absorption spectra of an ethanolic solution of pyrene in the presence of indole as a function of the photolysis time. [Indole] = 0.3 M and $\lambda_{ir} = 334 \text{ nm}$.

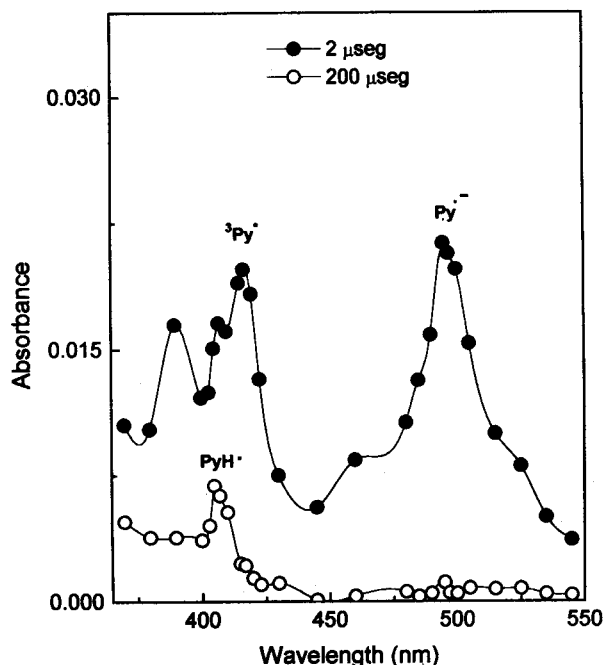


Figure 5. Transient absorption spectra of pyrene-indole 0.3 M in acetone after a laser pulse at 337 nm.

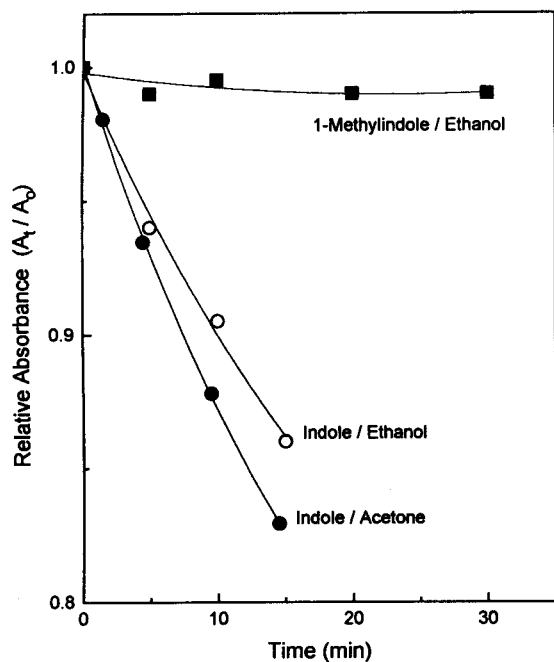


Figure 6. Continuous photolysis at 334 nm of pyrene in the presence of indoles in acetone and ethanol. Relative absorbance of the pyrene longest wavelength band vs. time. [Indoles] = 0.3 M.

phase in a similar way to that proposed for the system pyrene-*N,N*-dimethylaniline¹¹. On the other hand, the inhibitory effect of SDS and the very low yield of radical ions may be explained by the negative interface which retains the radical ion of the indole, while the more hydrophobic pyrene radical anion remains more deeply located in the

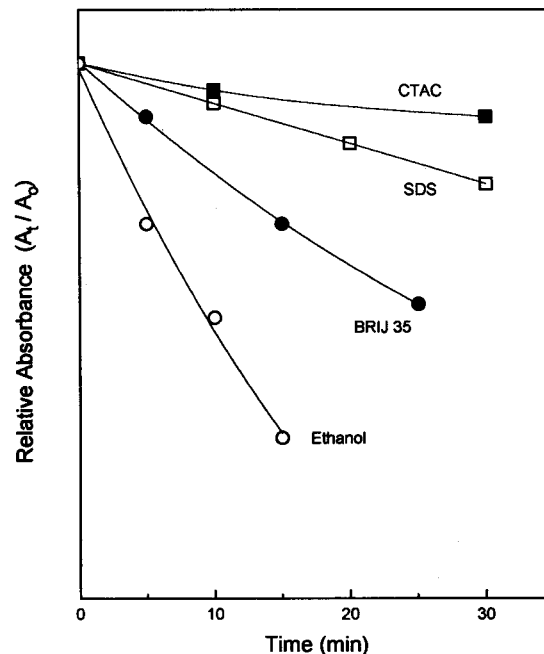


Figure 7. Micellar effect on the photolysis of pyrene-indole. [Surfactant] = 0.08 M. Indole concentration was such that more than 90% of the excited singlets were intercepted.

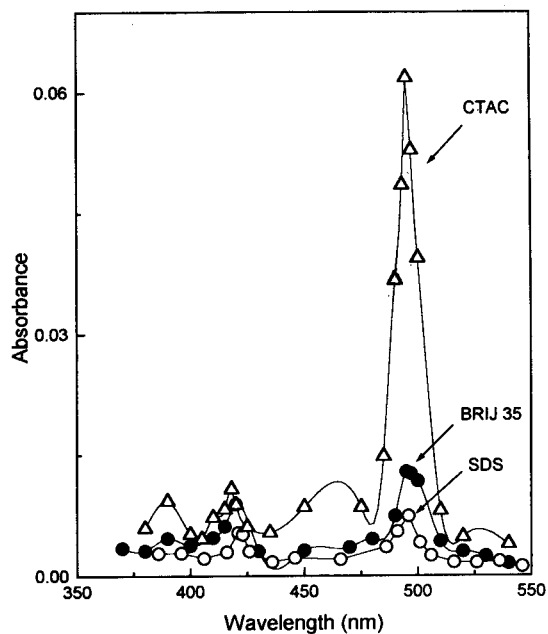


Figure 8. Transient absorption spectrum at 1 μ s after the laser pulse of the system pyrene-indole in micellar solutions.

micellar core. In this way the separation distance of the radical ions may be larger than that in homogeneous solvents. Now, it is well known that proton transfer in the geminate ion pair requires a close separation of the ions. Therefore, proton transfer may be inhibited but back-electron transfer may still be very efficient at this larger separation. In this way, within the time resolution of our

experiments ($\sim 1\mu\text{s}$) free radical ions may not be observed and at the same time the photobleaching may be reduced. In the similar system pyrene-*N,N*-dimethylaniline in SDS, a very fast initial decay of the radical ions (~ 200 ns) was also observed by Waka *et al.*¹¹ A confirmation that the inhibitory effect of CTAC and SDS is due to the charged interface is given by the lack of such effect for the neutral Brij-35 micelles.

Reverse micelles effect on the pyrene-indole system

The study of photophysical and photochemical processes in reverse micelles has received considerable attention during the last years¹². Reverse micelles can provide three different sites for location of small probe molecules, *i.e.*, the water pool, the interface of amphiphilic molecules and the organic phase. In previous work we have studied the distribution of indolic compounds¹³ and of pyrene derivatives¹⁴ in reverse micelles of AOT. Here we present results on the quenching of Py and derivatives by indolic compounds in reverse micelles of AOT in *n*-heptane.

Within the lifetime resolution of our experimental setup, the fluorescence decay of the pyrene derivatives in the reverse micelles, in the absence and in the presence of the indoles, appears as monoexponential in most cases. Therefore, a treatment similar to that in homogeneous solutions was applied. The data were plotted according to Eq. 1 in Figs. 9 and 10 for two different probes. The solutions were made with a water content parameter $R = 30$ ($R = [\text{H}_2\text{O}]/[\text{AOT}]$). The slope of these plots can be taken as a measure of the quenching efficiency for each system. The quenching of PBTMA by 2-MI and tryptamine is shown in Fig. 9. PBTMA is a cationic probe which is localized at the interface between the organic solvent and the water pool in the micellar system. 2-MI is a hydrophobic molecule that is preferentially solubilized in the organic phase, while tryptamine is known to be at the negative interface¹³. It can be seen that for the case of the quencher in the organic phase, similar slopes are obtained for the case of the reverse micellar system or a homogeneous system. On the other hand, for the quencher localized in the interface it can be seen that the quenching efficiency is very much less in the reverse micellar system. However, in this case a much higher local concentration in this region is expected. Similar results were obtained when the other positive probe PMTMA was employed. In Fig. 10 the results for the negative probe PSA are shown. The plots are very much like those in Fig. 9 for the positive probe. It was previously reported that for monocharged hydrophobic ions like pyrene derivatives, the location of the ring is independent of the charge^{15a}, and that it can be considered to remain mainly at the interface. Therefore, although PSA bears the same charge than the detergent molecules it is also believed to be located at the interface^{15b} up to $R = 30$, most probably co-micellizing with the surfactant molecules.

Here again a lower efficiency is observed when the quencher is at the interface in spite of its much higher local concentration. These results can be explained by a very much rigid structure of the interface, or by a very low mobility of the quencher and probe due to the binding to the interface. These two possibilities are related, since a

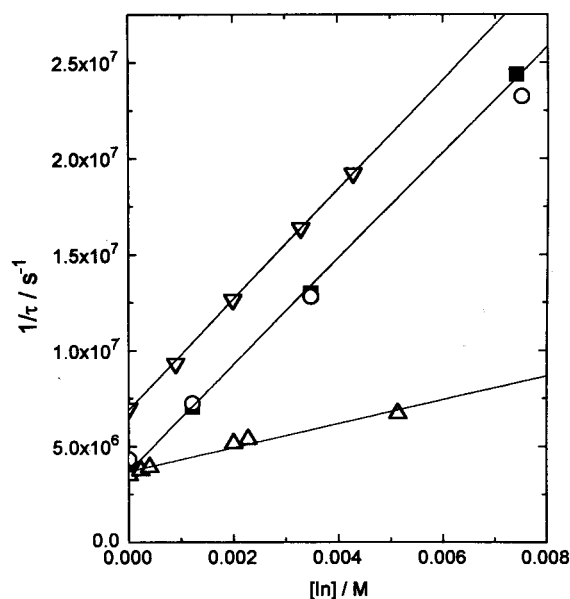


Figure 9. Quenching of PBTMA by 2-Methylindole and tryptamine in homogeneous and reverse micelles solutions. (■) 2-MI in EtOH; (○) 2-MI in AOT-heptane $R = 30$; (▽) tryptamine in water; (△) tryptamine in AOT-heptane $R = 30$.

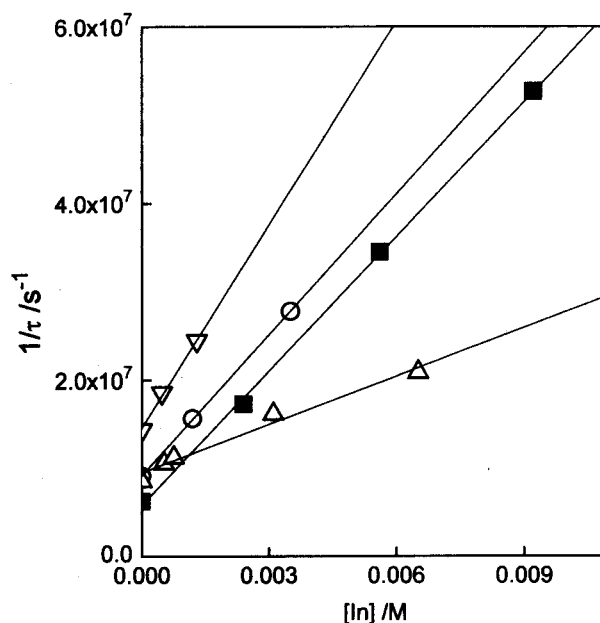


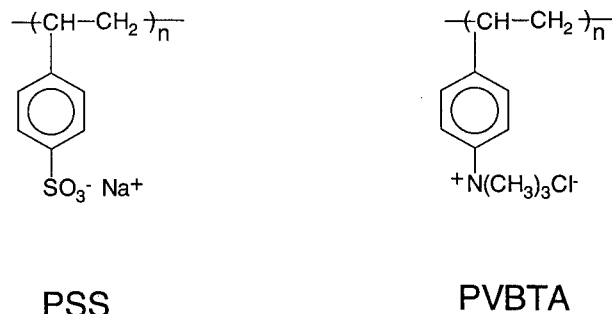
Figure 10. Quenching of PSA by 2-Methylindole and tryptamine in homogeneous and reverse micelles solutions. (■) 2-MI in EtOH; (○) 2-MI in AOT-heptane $R = 30$; (▽) tryptamine in water; (△) tryptamine in AOT-heptane $R = 30$.

certain degree of rigidity implies a high viscosity and therefore a lower mobility. Further studies are in progress in our laboratory in order to check this point.

Polyelectrolytes effect on the pyrene-indole system

Polyelectrolytes have been widely used to accelerate bimolecular photochemical reactions by making use of the high local concentration of reactants that may be achieved in the polyion charged interface. In the particular case of photoinduced electron transfer reactions, polyelectrolytes have been employed with the aim of optimizing the charge separation yields. We will now discuss the effect of polyelectrolytes on the electron transfer quenching of pyrene by indoles. Two polyelectrolytes were employed sodium poly(styrene sulfonate) (PSS, molecular weight 5×10^5) and poly(vinyl benzyl trimethylammonium) chloride (PVBTA, molecular weight 3×10^5). The structural formulas are shown in the Scheme 3.

The quenching of the positive probe PBTMA in the negative polyelectrolyte PSS by the neutral quencher indole, and by the positive one tryptamine, were investigated by static and dynamic fluorescence quenching. In Fig. 11 the results are shown for the system PBTMA-In-PSS. It can be seen that the quenching is lower in the presence of the polyelectrolyte. This is most likely due to the quenching taking place in an environment less polar than water. In a previous paper we have shown that PBTMA strongly interacts with PSS.¹⁶ At the polyelectrolyte concentration here employed near all the pyrene derivative will be incorporated in the polyion domain. These domains have a lower polarity as reflected by the absorption and fluorescence properties of the probe. Therefore, since the quenching rate constant decreases when the solvent polarity decreases, a lower quenching is expected in the polymer domain. The apparent quenching rate constants are collected in Table 2 (the concentration of the polyelectrolyte is expressed as normality, in terms of the charged monomer units). We have also study the interaction of indole derivatives with anionic and cationic polyelectrolytes¹⁷. It was found that while tryptamine is incorporated to the domain of PSS, neutral indole or tryptophan do not show any special affinity for the polyions. This difference is reflected in the quenching behavior of these indoles derivatives. The quenching by tryptamine is shown in Fig. 12 in the form of Stern-Volmer plots. In the presence of PSS at very low concentrations of the quencher both the static and dynamic contributions to the quenching show a great enhancement with respect to water. In Table 2 the dynamic quenching rate constants of tryptamine and tryptophan are collected. For the latter the apparent rate constants are very similar in the absence and the presence of the polyion, reflecting the small interaction of the aminoacid with the polymer. Similar explanation can be given to the results regarding the quenching of PSA in the presence of the cationic polyelec-



Scheme 3.

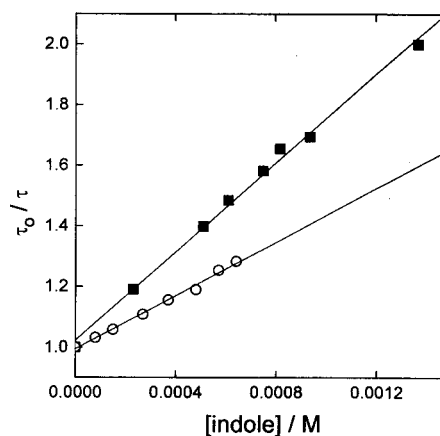


Figure 11. Stern-Volmer plot for the quenching of PBTMA by indole in water (■) and in the presence of PSS 0.02 N (○).

Table 2. Dynamic quenching rate constants of pyrene derivatives by indoles in the presence of polyelectrolytes.

Pyrene derivative	medium	indole derivative	$k_q / \text{M}^{-1} \text{s}^{-1}$
PBTMA	water	indole	5.2×10^9
PBTMA	PSS 0.01 N	indole	2.7×10^9
PBTMA	PSS 0.02 N	indole	2.7×10^9
PBTMA	water	tryptamine	2.8×10^9
PBTMA	PSS 0.01 N	tryptamine	2.9×10^{10}
PBTMA	water	tryptophan	3.3×10^9
PBTMA	PSS 0.01 N	tryptophan	2.1×10^9
PSA	water	indole	9×10^9
PSA	PVBTA 0.01 N	indole	2.5×10^9
PSA	water	tryptamine	1.0×10^{10}
PSA	PVBTA 0.01 N	tryptamine	1.0×10^8
PSA	water	tryptophan	4.7×10^9
PSA	PVBTA	tryptophan	4.7×10^8

trolyte PVBTA. Now the pyrene derivative is incorporated to the domain of the polyion and the quenching by the positive tryptamine is greatly diminished.

The transient absorption spectrum of PBTMA dissolved in PSS 0.01 N in the absence and in the presence of tryptamine 0.005 M is shown in Fig. 13. Under these conditions all the PBTMA ions are in the polymer domain and essentially all the excited singlets are intercepted by the quencher (see Fig. 12). However, the spectrum shows only the bands corresponding to the triplet state of the probe. That is, when the reaction takes place with both reactants incorporated to the polymer domain, free radical ions do not escape from cage recombination. From the intensity of the band in the presence of tryptamine it can be concluded

that the recombination reaction leads in part to the excited triplet of PBTMA.

In summary, the results here presented show that the electron transfer quenching between pyrene and indole is very sensitive to the medium both in the forward rate constant and in the charge separation efficiency. The latter, as well as the photochemical reaction which in some cases takes place, can be controlled by producing the reaction in organized systems. Normal micelles and polyelectrolytes seem to be the systems with better possibilities to allow a control of the photochemistry.

Acknowledgments

The financial support from Consejo Nacional de Investigaciones Científicas y Técnicas (CONICET), Consejo de Investigaciones Científicas y Tecnológicas de la Provincia de Córdoba (CONICOR) and Secretaría de Ciencia y Técnica de la Universidad Nacional de Río Cuarto, is gratefully acknowledged.

References

1. J.P. Palmas, M. Van der Auweraer, A.M. Swinnen and F.C. De Schryver, *J. Am. Chem. Soc.* **106**, 7721 (1984).
2. H.A. Montejano, J.J. Cosa, H.A. Garrera and C.M. Previtali, *J. Photochem. Photobiol. A: Chem.* **86**, 115 (1995).
3. N. Miyoshi and G. Tomita, *Photochem. Photobiol.* **29**, 527 (1979).
4. M.V. Encinas and E.A. Lissi, *Photochem. Photobiol.* **42**, 491 (1985).
5. M.V. Encinas and E.A. Lissi, *Photochem. Photobiol.* **44**, 579 (1986).
6. R.A. Marcus and N. Sutin, *Biochim. Biophys. Acta* **811**, 265 (1985).
7. N. Sutin, *Acc. Chem. Res.* **9**, 275 (1982).
8. M. Eigen, *Z. Phys. Chem. NF* **1**, 176 (1954).
9. N. Mataga, T. Asahi, Y. Kanda, T. Okada and T. Kakitani, *Chem. Phys.* **127**, 249 (1988).
10. T. Okada, N. Tashita and N. Mataga, *Chem. Phys. Lett.* **75**, 220 (1980). Y. Hirata, T. Saito and N. Mataga, *J. Phys. Chem.* **91**, 3119 (1987).
11. Y. Waka, K. Hamamoto and N. Mataga, *Photochem. Photobiol.* **32**, 27 (1980).
12. For a review of early work see K. Kalyanasundaram, *Photochemistry in Microheterogeneous Systems* (Acemic Press, New York, 1987).
13. S.G. Bertolotti, J.J. Cosa, C.M. Previtali, M.V. Encinas and E.A. Lissi, *Photochem. Photobiol.* **51**, 53 (1990). M.V. Encinas, E.A. Lissi, S.G. Bertolotti, J.J. Cosa and C.M. Previtali, *Photochem. Photobiol.* **52**, 981 (1990).

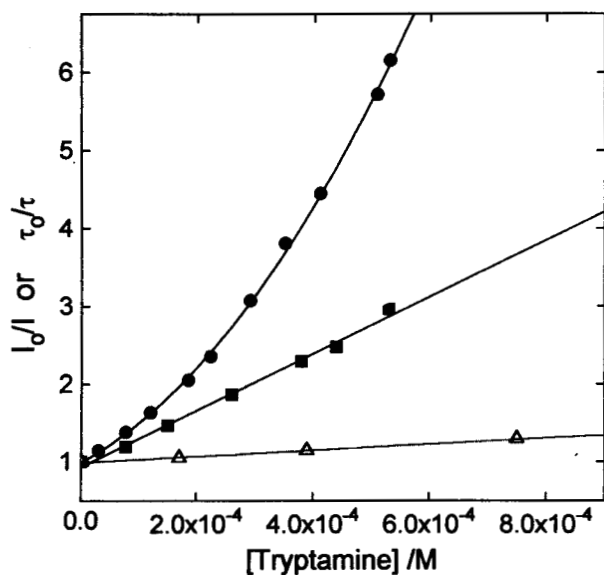


Figure 12. Static and dynamic Stern-Volmer plots for the quenching of PBTMA by tryptamine in water (Δ , τ_0/τ) and in the presence of PSS 0.01 N (\blacksquare , τ_0/τ ; \bullet , I_0/I).

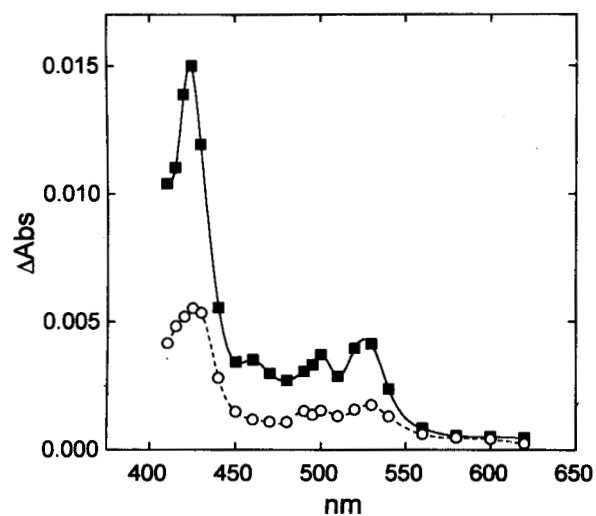


Figure 13. Transient absorption spectrum of PBTMA-PSS 0.01 N in the absence (\blacksquare) and the presence of tryptamine 0.005 M (\circ) taken 1.5 μ s after the laser pulse at 337 nm.

14. C.D. Borsarelli, J.J. Cosa and C.M. Previtali, *Langmuir* **8**, 1070 (1992).
15. (a) M. Sáez, E.A. Abuin and E.A. Lissi, *Langmuir* **5**, 942 (1989). (b) M.V. Encinas, E.A. Lissi, C.M. Previtali and J.J. Cosa, *Langmuir* **5**, 805 (1989).
16. O.E. Zimmerman, J.J. Cosa and C.M. Previtali, *J. Macromol. Sci.-Pure Appl. Chem.* **A31**, 859 (1994).
17. O.E. Zimmerman, J.J. Cosa and C.M. Previtali, *Photochem. Photobiol.* **52**, 711 (1990).